Optimum Coupling of Travelling Waves in a 9.4T Whole-Body Scanner

F. Geschewski[1], J. Felder[1], and N. Shah[1,2]

[1]Institute of Neuroscience and Medicine 4, Forschungszentrum Jülich GmbH, Juelich, NRW, Germany, [2]Faculty of Medicine, Department of Neurology, RWTH Aachen University, Aachen, Germany

Introduction: Following the proof-of-principle of the travelling wave concept on a 7T scanner [1], we investigate the installation of a travelling wave system on a 9.4T whole-body scanner. The system Larmor frequency is 399.68 MHz. Given the absence of a body coil, we wish to employ the integrated radiofrequency screen as a circular waveguide. The length and the inner diameter of the screen are 1220 mm and 684 mm respectively. For an air-filled circular waveguide with these dimensions, the dominant TE_{11}- and the TM_{01}-modes with the cut-off frequencies of 256.7 MHz and 335.5 MHz can be excited [2]. The excitation for MRI should create a homogenous H_1^+ field in the waveguide. Thus, two orthogonal TE_{11}-modes, with a phase shift of 90 degree, are used. The excitation device is a circularly polarised patch antenna. In this work the coupled power and the H_1^+ field distribution in the waveguide are determined for different patch positions with respect to the waveguide. The influence of a load in the waveguide and the influence of a complete magnet model are also examined.

Methods: The front plane of the patch antenna designed in-house is a 225 mm square of copper sheet glued onto a 30 mm thick PMMA former. The ground plane of the antenna formed by a square of copper sheet is mounted onto a 5mm thick PMMA former. The width and the length of both PMMA formers is 320 mm. The gap between the PMMA formers is variable [1]. The antenna is fed at two points in the front plane forming a right angle with a point a little outside of the centre of the patch. This small displacement out of the centre of the patch was chosen to increase the decoupling between the ports. Both PMMA formers are slotted around the default radial position of the feed points at 66.6 mm. Thus, radial positions of the feeding points in a range of 56 mm to 76 mm are available to match the impedance of the 50 Ω feed lines. The feed lines are semi-rigid coaxial lines. The inner and outer conductors of the coaxial lines are soldered at the front plane and at the ground plane, respectively. The power flow of the propagating modes through, and behind, the waveguide is simulated by integrating the Poynting vector over transverse control planes. The first control plane is positioned 300 mm behind the opening of the waveguide. With this plane the coupled power P_{in} is defined. The second plane is positioned behind the waveguide at the far field distance of the patch. With the second control plane the radiated power P_{rad} can be determined. The total electrical power P_{tot} is limited to 2 W. Fig.1 shows the tested patch positions. For positions 1 through 4 and 8, the centre of the patch is centred on the rotation axis of the waveguide. At position 1 the distance between the patch and the opening of the waveguide relates to a quarter waveguide wavelength of the TE_{11}-mode. At position 3 and 4 the opening of the waveguide is arranged in the far field and in twice the far field distance of the patch. At position 8, slanted radiation into the waveguide is examined. For the positions 5 to 7, different displacements of the patch out of the rotation axis of the waveguide are investigated. These displacements are in the x- and y-direction with a value of ± 50 mm. For the simulations with a loaded waveguide, a spherical phantom filled with a composition of distilled water has been used. The diameter of the phantom is 170 mm. The assumed material parameters of the phantom are $\varepsilon_r = 81$, $\mu_r = 0.999991$, $\rho = 997.075$ kg/m^3 and $\sigma = 0.95$ S/m. For the complete magnet the cryostat with an open diameter of 900 mm and a length of 3720 mm was added to the simulation model. For all simulations the metallic structures are modelled as perfect electric conductors (PEC). The simulations are performed with the FIM method using Microwave Studio (CST GmbH, Germany). The patch antenna and the required quadrature transmit/receive switch are home-built and are works-in-progress.

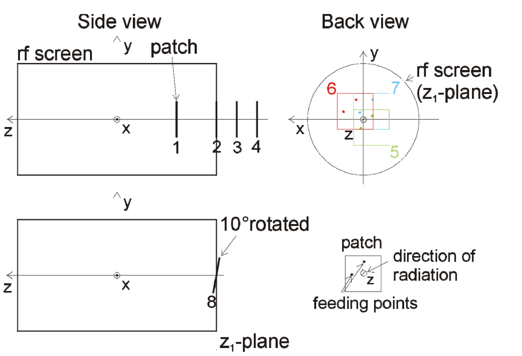

Fig.1: Tested patch positions (front plane of the patch)

Patch position	1	2	3	4	5	6	7	8
P_{in}/P_{tot} [%]	85.75	87.05	78.7	61.2	82.9	83.7	82.85	83.7
P_{rad}/P_{in} [%]	91.9	91.21	87.67	91.09	94.39	89.01	91.91	88.4

Tab.1: Coupled and radiated power for an unloaded waveguide

Results: For our simulations a return loss of both ports of better than 18 dB was achieved. The decoupling between the two ports was always better than 20dB. The results for the coupled and radiated power for an unloaded waveguide are listed in Table1. As one can see, the maximum coupled power was obtained at patch position 2. The lowest value occurred at patch position 4. This value of 61.2% is determined by free space losses between the patch and the waveguide. In contrast to the low level of the coupled power, the H_1^+ field distribution in the waveguide for patch position 4 was closest to the optimum case (compare Fig.2). In the ideal case the H_1^+ amplitude is independent of the direction of propagation (here z-direction) and the amplitude decreases with the radial distance from the centre of the waveguide. As one can see, in Fig.2 this ideal field distribution was not achieved. The major problem is the length of the waveguide, which is only a little longer than the waveguide wavelength of the TE_{11}-mode. Thus evanescence modes and reflections at the beginning and at the end of the waveguide create standing waves. With these standing waves local maxima of the H_1^+ amplitude at the beginning, the end, and a few millimetres behind the waveguide centre were generated (see Fig.2). The radial dependence of the H_1^+ amplitude was also disturbed. The best results for the combination of coupled power and field distribution were achieved with patch position 5 (see Fig.2 bottom). With the introduction of a load, the H_1^+ field distribution in the waveguide changed (see Fig.3 left). The propagating waves are reflected at the start and at the end of the load and they generate standing waves between the load and the waveguide terminations. For the 3 cases depicted in Fig.3, the coupled power was reduced by 2 % to 4 %. The H_1^+ field distribution over the load was similar and independent of the patch positions. Only the H_1^+ amplitude differed as a function of the coupled power. Simulations including the complete magnet model showed no significant differences in the field distribution. For the coupled power the differences between the loaded waveguide and the complete magnet model were lower than 1 %.

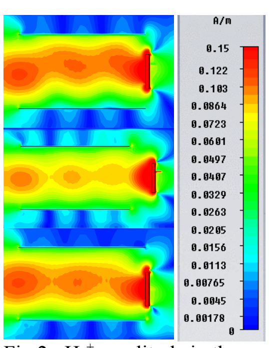

Fig.2: H_1^+ amplitude in the x-plane for the patch positions 2 (top), 4 (mid) and 5 (bottom)

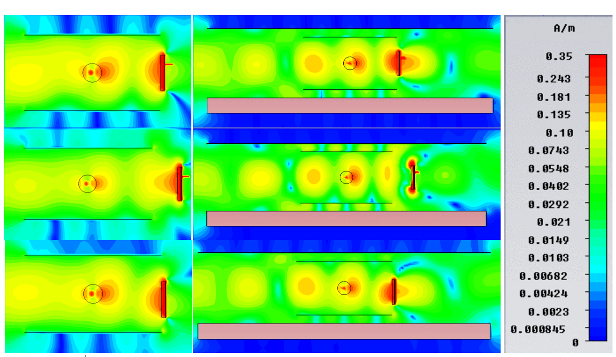

Fig.3: H_1^+ amplitude in the in the x-plane with a loaded waveguide (left side) and with a load in the complete magnet model for the patch positions 2 (top), 4 (mid) and 5 (bottom)

Conclusion: To couple the maximum power into the waveguide the patch antenna must be positioned directly at the beginning of the RF shield. An equal displacement in the x- and y-direction (see patch position 5 in Fig.1) of the patch can produce a field distribution that is more homogeneous. However this result depends on the antenna design and must be checked for every new kind of antenna.

References:

[1] Brunner et al "Travelling-wave nuclear magnetic resonance", Nature, vol. 457, p. 994-998 (2009).

[2] D.M. Pozar "Microwave Engineering", J. Wiley and Sons, INC., second ed., 1998.